A | R | J
Amrit Research Journal December 2025, Vol. 6, Issue 1, 98-111
ISSN: 2738-9553
RESEARCH ARTICLE

In Silico Docking, Pharmacokinetic, and Toxicological Profiling of *Ziziphus budhensis* Leaves Phytochemicals as Potential Aldose Reductase Inhibitors

Samjhana Bharati[1,2], Nirmal Parajuli[1,2], Timila Shrestha[1,2], Binita Maharjan[1,2], Bishnu P. Marasini[2,3,4], Jhashanath Adhikari Subin[5], Hari Prasad Devkota[6], Stefano Dall' Acqua[7,*], Ram Lal (Swagat) Shrestha[1,2,3,*]

[1]Department of Chemistry, Amrit Campus, Tribhuvan University, Lainchaur, Kathmandu 44600, Nepal
[2]Kathmandu Valley College, Syuchatar Bridge, Kalanki, Kathmandu 44600, Nepal
[3]Institute of Natural Resources Innovation, Kalimati, Kathmandu 44600, Nepal
[4]Nepal Health Research Council, Ministry of Health and Population, Ramshah Path, Kathmandu 44600, Nepal
[5]Forest Biomaterials Science and Engineering, Institute of Applied Sciences, Madan Bhandari University of Science and Technology, Chitlang, Makawanpur 44100, Nepal
[6]Faculty of Humanities and Social Sciences, Kumamoto University, Kumamoto, Japan
[7]Department of Pharmaceutical and Pharmacological Sciences, University of Padova, Padova, Italy
**Email: stefano.dallacqua@unipd.it; swagatstha@gmail.com*

(Received: September 28, 2025, Received in revised form: November 21, 2025, Accepted: December 3, 2025, Available online: December 19, 2025)

DOI: https://doi.org/10.3126/arj.v6i1.87537

Highlights

- A structure-based virtual screening approach was used to evaluate the phytochemicals from *Ziziphus budhensis* leaves as potential aldose reductase (AR) inhibitors
- Two compounds (Epicatechin and Catechin) showed higher binding affinities, improved pharmacokinetic properties, and a lower toxicity profile compared with the native inhibitor Zenarestat
- Molecular interaction analysis revealed multiple hydrogen bonding and hydrophobic interactions with key active-site residues of AR
- The study reveals a computational foundation for developing natural, plant-based AR inhibitors to manage diabetic complications

Abstract

Diabetes mellitus is a long-term metabolic disorder associated with hyperglycemia-induced complications, mostly regulated through aldose reductase (AR), a key enzyme in the polyol pathway. Therefore, inhibition of AR has become an emerging therapeutic strategy to manage diabetes-associated complications linked to carbohydrate metabolism. In this study, 29 phytochemicals from Ziziphus budhensis leaves were computationally screened against AR enzymes (PDB ID: 1IEI) using molecular docking and pharmacokinetic analysis. Among the screened compounds, Eriodictyol-7-O-glucoside (M01), Epicatechin (M02), Euscaphic acid (M03), and Catechin (M04) exhibited the highest binding affinities with docking scores of -11.3, -10.3, -10.1 and -9.9 kcal/mol, respectively, exceeding that of the native inhibitor Zenarestat (-9.7 kcal/mol). These compounds showed multiple hydrogen-bond interactions with key active-site amino acid residues, suggesting strong and favourable binding interactions in the polyol pathway. The ADMET profile of these hit molecules highlighted that compounds M02 and M04 possess the best drug-

**Corresponding author*

likeness, oral bioavailability, and balanced physicochemical properties, and the least toxic characteristics, compared to native and other top ligands, strengthening their potential as safe and effective AR inhibitors. Therefore, the molecules M02 and M04 are recommended as possible AR inhibitors, based on docking and pharmacokinetic predictions. This study facilitates a good theoretical foundation for developing plant-based inhibitors targeting AR for diabetes management.

Keywords: *Ziziphus budhensis, aldose reductase, molecular docking, pharmacokinetics, toxicity*

Introduction

Natural products have been a major source of therapeutic agents since ancient times, and they continue to play a vital role in modern drug discovery (Arnold & Lixin, 2019). Various activities, such as hypoglycemic, antioxidant, anti-inflammatory, and hepatoprotective, have been reported for phytochemicals isolated from several medicinal plants (Butler, 2004). Due to multiple modes of action targeting different molecular targets, several compounds have been recognised as potentially applicable for diabetes or its complications. Enzymatic activities are involved in diabetic disease, and natural compounds that act as enzyme inhibitors can serve as new potential antidiabetic drugs. Enzymatic activities evaluated in the discovery of new antidiabetic drugs include alpha-glucosidase, amylase, and aldose reductase. Additionally, compounds that reduce oxidative stress and, consequently, the formation of Advanced Glycation End-products (AGEs) could play a good role in this regard. Along with that, compounds that can lower plasma glucose levels by targeting hexokinase and glucose-6-phosphate, or influencing the synthesis and release of insulin from pancreatic beta cells, reducing the glucose absorption, or promoting the glucose consumption and absorption by interacting with transporters as GLUT4, may also be considered in the future as potential new candidates (Alam et al., 2019).

Plants can be considered a good source of antidiabetic agents, and research can begin to objectify the folkloric and traditional medicines. Traditional herbal medicines are widely regarded for their potential in treating diabetic syndromes due to their mechanisms of action, including insulin secretion and sensitivity, glucose uptake by muscle cells and adipose tissues, and inhibition of glucose absorption (Alam et al., 2022). It forms the basics for utilising such concept in this research work.

Diabetes mellitus is a long-term metabolic disorder associated with hyperglycemia due to impaired insulin secretion, insulin action, or both (Nauck et al., 2021). It persists as one of the most prevalent metabolic diseases globally and is responsible for the multiple chronic complications affecting the kidneys, nerves, eyes, and cardiovascular system (Pasquel et al., 2021). The polyol pathway plays a central role among the many biochemical mechanisms involved in hyperglycemia-induced complications(Gupta, 2024). The first and rate-limiting enzyme of this pathway, aldose reductase (AR), catalyses the nicotinamide adenine dinucleotide phosphate (NADPH)-dependent reduction of glucose to sorbitol (Del-Corso et al., 2013). The polyol pathway aids glucose metabolism under normal physiological conditions and maintains osmotic balance.

On the other hand, during hyperglycemia, excessive activation of these pathways leads to intracellular accumulation of sorbitol and fructose, resulting in osmotic stress, tissue damage, and oxidative imbalance (Ramasamy & Goldberg, 2010). Therefore, the excessive expression of AR has been linked to diabetes-mediated pathologies such as nephropathy, neuropathy, retinopathy, and cataract formation (Ramasamy & Goldberg, 2010). Hence, AR inhibition has emerged as a promising therapeutic approach to moderate secondary diabetic complications by restoring normal carbohydrate metabolism and preventing oxidative stress.

The emergence and advancement of bioinformatics and cheminformatics have developed new avenues for accurately and efficiently exploring molecular interactions (Shrestha et al., 2025a). Traditional drug discovery and screening methods can be expensive, time-consuming, and require extensive laboratory experiments (Subin & Shrestha, 2024). Computational techniques such as molecular docking and pharmacokinetics offer an efficient alternative to predict possible biological activities and assess molecular behavior at the atomic scale (Shrestha et al., 2025b) These approaches help in the identification of possible hit molecules and open a direction in the understanding of their binding interaction with the target protein before the experimental validation (Kitchen et al., 2004). Molecular docking is one of the most widely used, reliable, and robust techniques for structure-based drug discovery. It predicts the preferred orientation of a ligand when docked to a protein's active site and calculates the binding affinity through scoring functions (Shrestha et al., 2025c). Thereupon, molecular docking provides preliminary, valuable insights into the binding mechanism, interacting residues, and the overall binding pattern in the protein-ligand complex. The ribbon structure of the AR enzyme with the co-crystal ligand Zenarestat is shown in Figure 1.

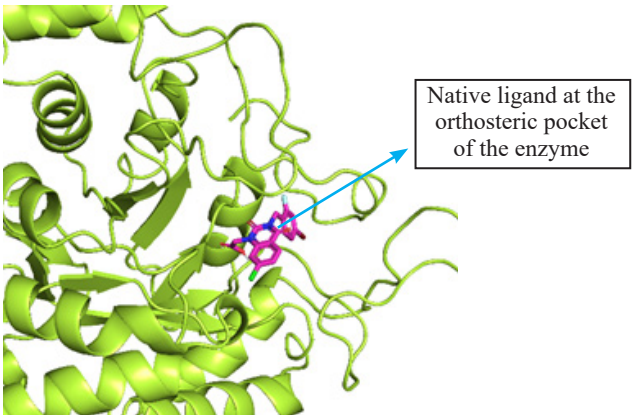

Fig. 1. Native ligand (Zenarestat) at the orthosteric pocket of the enzyme (PDB ID: 1IEI) in ribbon representation

To understand a compound's therapeutic viability, its pharmacokinetics and drug-likeness features must be evaluated (Cao et al., 2012). It is crucial to predict a compound's behaviour in living systems, including its absorption, distribution, metabolism, excretion, and toxicity (ADMET) characteristics (Daina et al., 2017). Such analysis aligns with the modern techniques of rational drug design, where *in silico* prediction serves as the first step toward identifying biologically active and pharmacologically favourable molecules.

This study aims to screen phytocompounds derived from *Z. budhensis* leaves as potential AR inhibitors using a computational approach and lay the foundation for further experimental verification, as no *in silico/in vitro* approach has been reported for AR inhibition screening of *Z. budhensis* phytocompounds yet. This work is a continuation and extension of previous work on *Z. budhensis* leaves (Bharati et al., 2025) that aimed to identify multiple phytoconstituents and to observe the enzyme-inhibitory properties of some of the obtained extracts.

Materials and Methods

Selection and Preparation of Ligands

Twenty-nine phytocompounds from *Z. budhensis* leaves reported by Bharati et al., characterised through LC-DAD-MS^n and HR-LC-QTOF, were selected as ligands (Table 1) (Bharati et al., 2025). The PubChem database (Kim et al., 2023) and the Coconut database (Chandrasekhar et al., 2025) were used to retrieve the 3D structures of the ligands in SDF format. Structural optimisation was performed using the Avogadro program (version 1.2.0) (Hanwell et al., 2012) with the Universal Force Field (UFF) for 5000 steps, a conjugate gradients algorithm, and a convergence threshold of 10−8 kcal/mol, set to reach the global minimum. It was then saved in PDB format. After that, the ligands were converted to PDBQT format with the addition of Gasteiger charges using the AutoDock Tools (Trott & Olson, 2009).

Protein structure preparation

The human aldose reductase enzyme crystal structure (PDB ID: 1IEI) (https://doi.org/10.2210/pdb1IEI/pdb) with 2.50 Å resolution, characterised by X-ray diffraction, and expressed in *Escherichia coli,* was retrieved from the RCSB protein database (Berman et al., 2000). Preparation and visualisation of the protein structure were done using the PyMOL program (v 2.2.5) and AutoDock Tools v1.5.7 (Trott & Olson, 2010; Yuan et al., 2017). The protein structure was further processed by removing ions, water molecules, and the co-crystallised ligand (ZES), along with other non-standard residues, and saved in PDB format as the apo protein structure. Using the AutoDock Tools, polar hydrogen and Kollman charges were added. Finally, it was saved in pdbqt format, which is used in molecular docking calculations.

Molecular Docking Calculation Parameters

Molecular docking was performed using AutoDock Vina v1.1.2 (Trott & Olson, 2010) to identify the optimal ligand binding pose within the enzyme's binding site. Binding affinities were evaluated with a specified scoring function in AutoDock Vina. The grid centre for docking was chosen (x: -3.821, y: 0.868, z: 7.852) with a box size of 38 × 38 × 36 $Å^3$ covering all the binding

pocket of the target enzyme. The control parameters, exhaustiveness of 32, energy range of 4, and 20 docking modes for docking protocol validation were applied to the co-crystallised native ligand for RMSD calculation, which was later applied for docking calculation of all selected ligands with the target. The predicted binding affinities could be considered as the known limitations of the AutoDock Vina scoring function, particularly its simplified treatment of entropic contributions, solvation effects, and long-range interactions. The outputs were observed with programs PyMOL and Biovia Discovery Studio (v 20.1.0.23289) (D.S., 2021).

Pharmacokinetic and Pharmacodynamic Evaluations

The SwissADME server-based tool was used to predict the pharmacokinetic properties of top-docked candidates (https://www.swissadme.ch/) (assessed on November 1, 2025) (Daina et al., 2017). It provides an integrated platform for evaluating key physicochemical and pharmacokinetic parameters, including molecular weight, lipophilicity, solubility, and bioavailability. In biological systems, these parameters are crucial for predicting the compound's behaviour, including its absorption, distribution, metabolism, and excretion (ADME) characteristics. Additionally, the *in silico* toxicity evaluation of the hit phytocompounds with the reference inhibitor (native) Zenarestat was performed using the ProTox-III server (https://tox.charite.de/protox3/) to predict acute toxicity (LD_{50}), toxicity class, and organ-specific liabilities (hepatotoxicity, nephrotoxicity, neurotoxicity, cardiotoxicity, immunotoxicity, mutagenicity, cytotoxicity, and toxicity to the BBB-barrier) (Banerjee et al., 2024).

Results and Discussion

Protocol validation and molecular docking calculation

The docking protocol was authenticated by calculating the root mean square deviation (RMSD) of less than 2 A (0.317 Å) between the heavy atoms of the co-crystallised ligand (Zenarestat) in the protein structure and the docked native ligand obtained from calculation (Shrestha et al., 2024). The superimposed geometry of the co-crystallised ligand and docked ligand is presented in Figure 2.

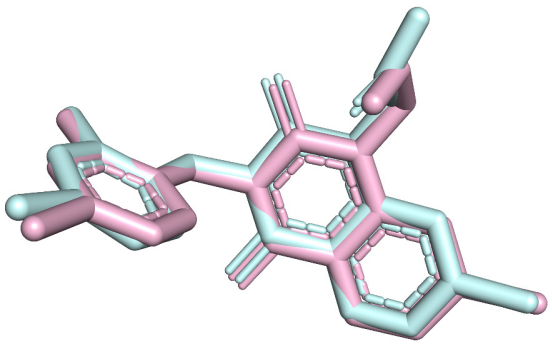

Fig. 2. The superimposed structure of co-crystal ligand (light pink) and docked native ligand (light blue) with heavy atom RMSD of 0.317 Å

The compounds identified by LC-DAD-MS^n and HR-LC-QTOF characterisation were screened for AR inhibition using molecular docking.

Table 1. Selected compounds with identification numbers and docking scores

Ligands	Name of compound	Identification number	Docking score (kcal/mol)
M01	Eryiodichtiol-7-O-glucoside	13254473	-11.3
M02	(-)-Epicatechin	72276	-10.3
M03	Euscaphic acid	471426	-10.1
M04	Catechin	9064	-9.9
M05	Oxiphylline A	-	-9.7
M06	Maslinic acid	73659	-9.6
M07	Oleanolic acid	10494	-9.4

M08	Pomolic acid	382831	-9.1
M09	Juzirine	3085285	-9.1
M10	quercetin-dirhamnoside	15953752	-9.0
M11	Annocherine A	22297560	-8.9
M12	Zinziphin	CNP0364507.1	-8.8
M13	Medicagenic acid	65048	-8.6
M14	Ziziberanalic acid	21672700	-8.6
M15	Mauritine F	57402357	-8.6
M16	Jujubasaponin IV	73204032	-8.5
M17	Quercetin-3-O-glucoside	5280804	-8.4
M18	Protocatechuic acid glucoside	91309592	-8.4
M19	Quercetin-3-O-rhamnoside	5280459	-8.4
M20	Kaempferol-3-O-rutinoside	5318767	-8.4
M21	Quercetin-3-O-rutinoside	5280805	-8.3
M22	Isoboldine	133323	-8.2
M23	Boldine	10154	-8.2
M24	Ceanothic acid	161352	-8.2
M25	Kaempferol-3-O-β-neohesperidoside	5318761	-7.9
M26	Spinosin	155692	-7.9
M27	Quercetin 3-O-β-neohesperidoside	5491657	-7.6
M28	Hovenine A	5318090	-7.6
M29	Isospinosin	11801844	-7.4
Native	*Zenarestat	5724	-9.7

Here, ID with prefix CNP: taken from the Coconut database, IDs with no prefix: PubChem database, with no ID: Drawn from Chemdraw 16, and *: Native ligand

Table 1 lists all selected phytochemicals, their respective identification numbers from two databases, and docking scores. Four of the selected ligands exceeded the docking score of native Zenarestat (-9.7 kcal/mol). Molecule M01 scored the highest binding affinity with -11.3 kcal/mol. The other top three ligands, M02, M03, and M04, scored -10.3, -10.1, and -9.9 kcal/mol, respectively. Overall, the four ligands were identified as top compounds targeting the enzyme AR, based on their binding affinity and potential to modulate its normal function.

Molecular-level interactions in the adducts

A comprehensive illustration of the interactions between the top four ligands and native with aldose reductase enzyme is summarised in Table 2. Interactive pictures containing interaction distance (Å) between ligand and amino acid residues are presented in Figure 3.

Table 2. Ligand structures, types of interactions, and responsible amino acid residues with distances of the top four ligands, and native complexed with the aldose reductase enzyme

Ligands	**Types of Interactions**	**Amino acid residues with distances (Å)**
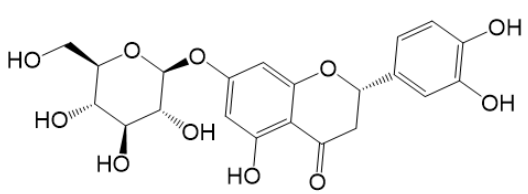 **M01**	Conventional Hydrogen Bond	LYS21 (2.14), ASP43 (2.69), LYS77 (2.90), ASP216 (2.29), CYS298 (2.23, 3.07)
	Pi-Pi Stacked	TYR209 (4.12)
	Pi-Donor Hydrogen Bond	LYS262 (3.16)
	van der Waals	THR19, HIS110, GLN183, TRP219

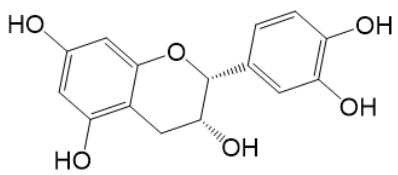 **M02**	Conventional Hydrogen Bond	LYS21 (2.06), ASP43 (2.98), LYS77 (2.67), ASP216 (2.33), LYS262 (3.09)
	Pi-Donor Hydrogen Bond	LYS262 (3.07)
	Carbon Hydrogen Bond	PRO215 (3.80), ILE260 (3.29)
	Pi-Alkyl	TYR209 (5.33)
	Pi-Pi Stacked	TYR209 (4.14)
	van der Waals	THR19, HIS110, GLN183
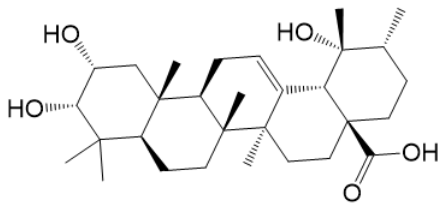 **M03**	Conventional Hydrogen bond	GLN49 (2.02)
	Pi-alkyl	TRP20 (4.95, 4.60), TRP111 (4.67), PHE122 (5.09), TRP219 (4.63)
	van der Waals	LYS21, VAL47, TYR48, HIS110, PHE121, CYS298
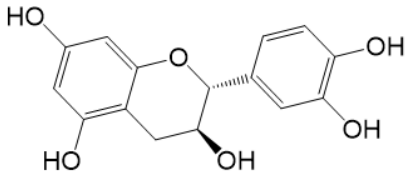 **M04**	Conventional Hydrogen bond	LYS21 (1.98), ASP43 (2.68), TYR48 (2.54) ASP216 (2.30), CYS298 (3.79)
	Carbon Hydrogen bond	GLY18 (3.25)
	Pi-Donor Hydrogen Bond	LYS262 (3.16)
	Pi-Pi Stacked	TYR209 (4.09)
	van der Waals	LYS77, HIS110, GLN183, PRO261
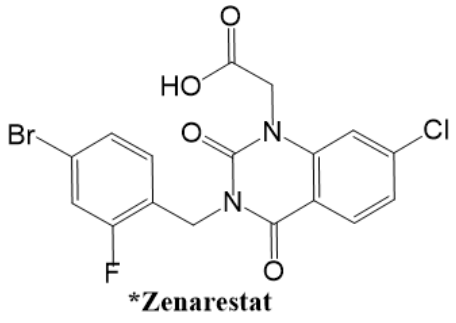 ***Zenarestat**	Conventional Hydrogen bond	TYR48 (1.97), HIS110 (2.11), TRP111 (2.11)
	Pi-Sigma	LEU300 (3.60)
	Pi-Pi Stacked	TRP20 (4.94, 5.00), TRP111 (3.83)
	Carbon Hydrogen Bond	CYS298 (3.38)
	Pi-alkyl	TRP20 (4.55)
	Halogen (Fluorine)	ALA299 (3.56), CYS298 (2.59)
	Alkyl	VAL47 (4.40), CYS80 (4.94), CYS303 (4.27)
	van der Waals	TRP79, TRP219, TYR309

M01: Eryiodichtiol-7-O-glucoside, **M02**: (-)-Epicatechin, **M03**: Euscaphic acid, **M04**: Catechin and *: Native ligand

AR has been characterised with the active-site residues, mainly HIS110, TYR48, TRP20, ASP43, LYS77, and TRP111, and by other surrounding residues that alter the enzyme's function (Ashika et al., 2022). A flavanone glycoside, Eryiodichtiol-7-O-glucoside, M01, was found to be bound with the target enzyme through six strong and moderate hydrogen bonds (H-bonds) with amino acid residues LYS21, ASP43, LYS77, ASP216, and CYS298, with bond distances in the range of 2.14 to 3.07 Å. Other supporting Pi-donor hydrogen bonds (LYS262), Pi-Pi stacked interaction (TYR209), and various surrounding amino acid residues were found to interact with the ligand M01 through van der Waals interactions (Figure 3). The multiple hydrogen bond interactions with active-site residues exhibited by M01 likely played a key role in the confined binding conformation within the binding pocket, thereby contributing to the highest docking score among the tested compounds (Xue et al., 2025).

The flavan-3-ol derivatives epicatechin and catechin, indicated as molecules M02 and M04, respectively, were found to interact with the target in a similar manner, likely due to their similar structural scaffold. They are stereoisomers, and both formed 5 H-bonds each, which might indicate their strong binding affinity towards the AR enzyme (Guedes et al., 2021). LYS21, ASP43,

and ASP216 formed strong H-bonds at bond distances below 3 Å in both. LYS77 and LYS262 formed additional H-bonds with M02, while two other H-bonds with M04 were found with amino acids TYR48 and CYS298. M02-enzyme complex was further characterised with other hydrophobic Pi-donor hydrogen bond (LYS262), carbon hydrogen bond (PRO215, ILE260), Pi-alkyl interactions, and van der Waals forces. A similar pattern of interactions was observed for the M04-enzyme complex. Carbon-hydrogen bond (GLY18), Pi-Pi stacked (TYR209), and van der Waals interactions were observed in addition to the hydrogen bond. It was observed that binding affinity and orientation of the molecule at the best docked position are related to the variation of the compound skeleton and configuration of the functional groups in a molecule, as analysed by the docking outputs of various classes of selected compounds (Xie & Hwang, 2010).

The triterpene acid euscaphic acid, which chemically can be considered as a polycyclic aliphatic acid and is indicated as M03, resulted in the formation of one strong H-bond with GLN49 at a bond distance of 2.02 Å, along with other supporting hydrophobic Pi-alkyl interactions with amino acid residues TRP20, TRP111, PHE122, TRP219, and van der Waals interactions. A pattern of M03-enzyme interactions, compared with other top ligands and the native ligand, clearly shows variation in interactions due to structural configuration and molecular scaffold. Interestingly, a good interaction is observed with M03 and appears to be structure-specific, as limited results were obtained with the other triterpenoids considered, namely medicagenic, maslinic, pomolic, and ziziberanalic acid (Bharati et al., 2025).

Native ligand (Zenerestat) is a synthetic AR inhibitor that was investigated as a treatment for pathophysiological consequences of diabetes, particularly diabetic neuropathy (Greene et al., 1999), and we considered this compound as a reference for the *in silico* evaluation. Molecular docking of the native ligand with AR was found to form three strong H-bonds with amino acid residues of the binding site TYR38, HIS110, and TRP111, with the interaction distance below 2.11 Å. It was complexed with AR through additional hydrophobic Pi-sigma (LEU300), Pi-Pi stacked (TRP20), Pi-alkyl (TRP20, TRP111), Halogen (ALA299, CYS298), alkyl (VAL 47, CYS80, CYS303), and van der Waals interactions. Such variation in the bond upon complex formation indicates molecular recognition of AR and effective binding at the binding pocket.

A comparative study of the interactions between the four top ligands and native Zenerestat with AR revealed differences in H-bond formation, hydrophobic interactions, and the involvement of key amino acid residues. Meanwhile, the binding pattern of the top ligands with the enzyme was found to be similar. The primary cause of this observation is the dissimilar spatial orientation and architectural variation in the ligand scaffold compared to the native ligand (Agu et al., 2023). The top candidates, native and both, were able to form good interactions with the active-site residues ASP43, LYS77, TYR48, and TRP111 through hydrophilic and hydrophobic interactions. Therefore, the four selected molecules were found to be the best candidates for binding to the target enzyme AR, owing to numerous strong H-bonds with active-site amino acid residues and a higher docking score than Zenerestat. Such interactions and binding modes of hit molecules could be predicted to yield better inhibitors that can modulate the functionality of the enzyme AR to control secondary hyperglycemic complications and sugar metabolism.

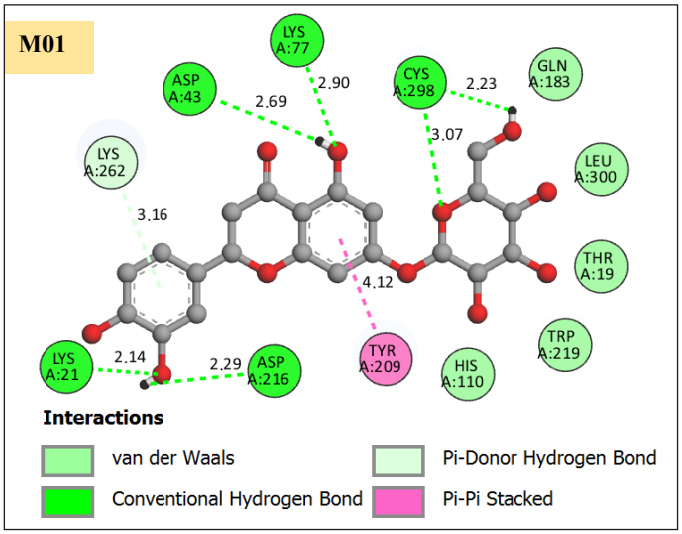

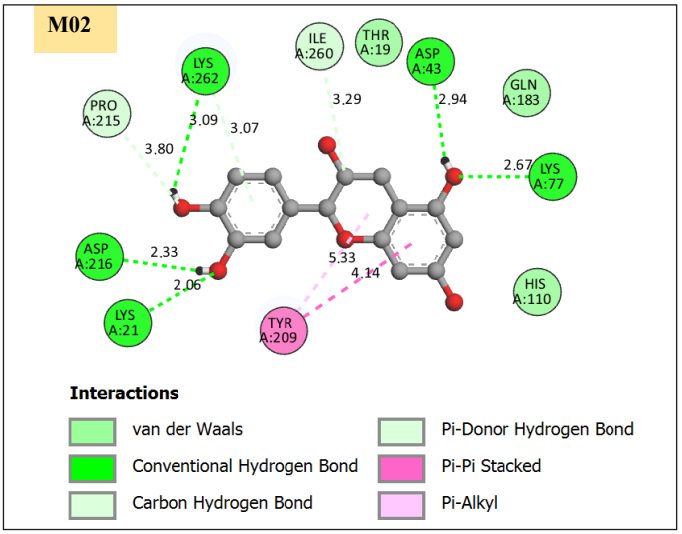

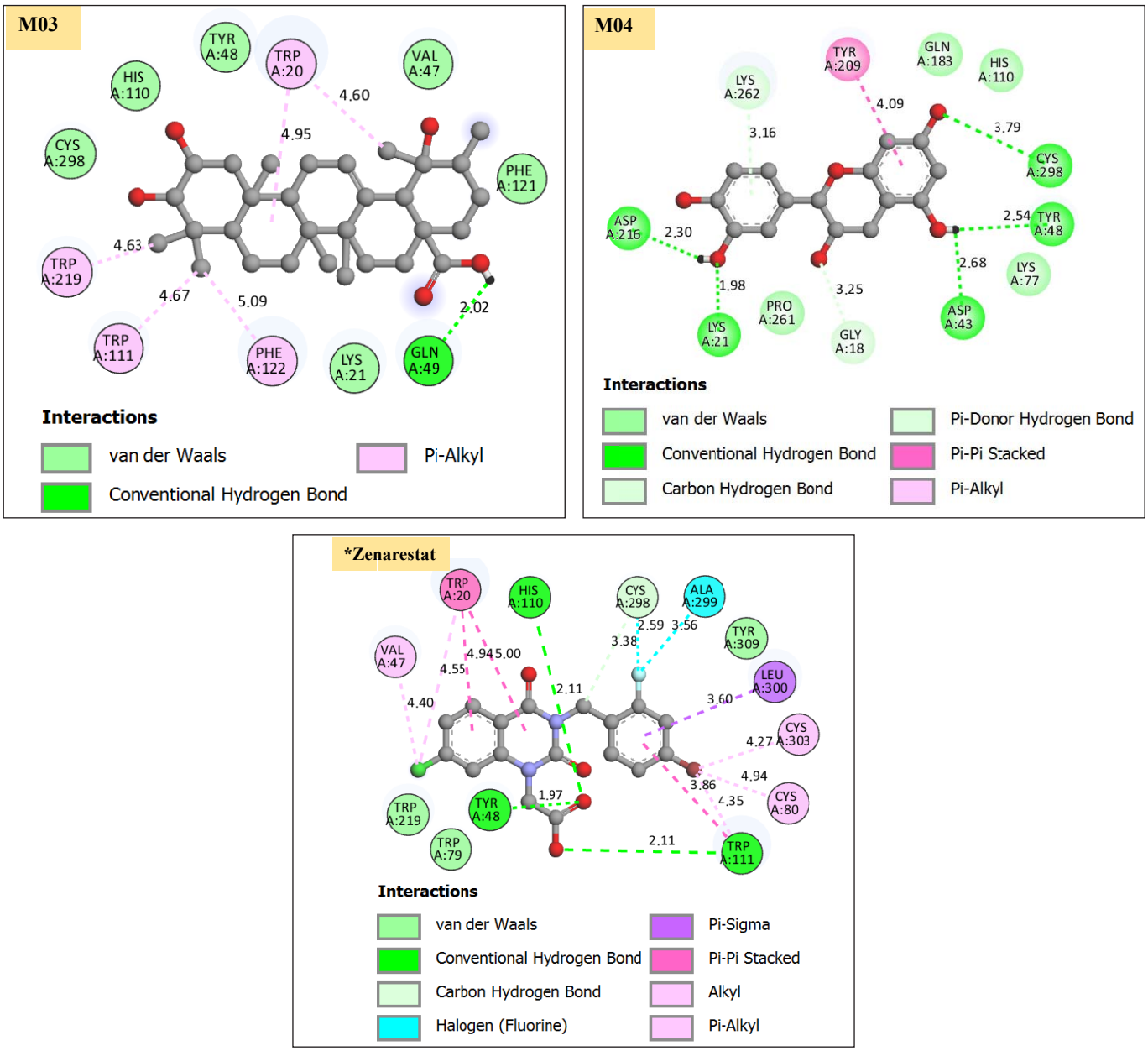

Fig. 3. 2D interactive presentation of top four ligands (M01, M02, M03, M04) and Native (*Zenarestat) at the best binding pose with the surrounding active site amino acid residues at the orthosteric site of the aldose reductase enzyme

Pharmacokinetics and Toxicity Analysis

The high failure rate of drug candidates in medical development is attributed mainly to suboptimal pharmacokinetic behaviour. Therefore, the evaluation of drug-likeness has become a key criterion in early-stage drug discovery, enabling the selection of compounds with promising bioavailability and developability (Hefti, 2008). A comprehensive physicochemical evaluation was performed to assess the oral drug-likeness and drug development potential of the top four phytocompounds relative to the reference inhibitor, Zenarestat. Key properties, including molecular weight, hydrogen-bonding capacity, topological polar surface area (TPSA), rotatable bonds, and lipophilicity, were analysed for their critical roles in permeability, solubility, and pharmacokinetic behaviour. Table 3 summarises these properties for the four selected phytocompounds alongside Zenarestat.

Table 3. Physicochemical properties of the top four compounds and the native ligand

Physicochemical Properties/Ligands	Eriodictyol-7-O-Glucoside (M01)	Epicatechin (M02)	Euscaphic Acid (M03)	Catechin (M04)	Native Ligand (Zenarestat)
Formula	$C_{21}H_{22}O_{11}$	$C_{15}H_{14}O_6$	$C_{30}H_{48}O_5$	$C_{15}H_{14}O_6$	$C_{17}H_{11}BrClFN_2O_4$
Molecular weight	450.39	290.27	488.7	290.27	441.64
Num. rotatable bonds	4	1	1	1	4
Num. H-bond acceptors	11	6	5	6	5
Num. H-bond donors	7	5	4	5	1
TPSA (Å²)	186.37	110.38	97.99	110.38	81.3
Lipophilicity Consensus Log Po/w	-0.32	0.85	4.34	0.83	3.35

From Table 3, we can see that all four compounds fell within the prime molecular weight range (<500 Da), comparable to the native ligand Zenarestat, suggesting their favourable potential for passive absorption. As per the physicochemical analysis, M01 showed a significantly high number of the hydrogen bond donors (7) and acceptors (11) at the same time with high topological polar surface area (TPSA=186.37 Å²), resulting in poor permeability and compromised oral absorption potential due to excessive polarity (Wang et al., 2021).

Although M01 exhibited strong docking affinity, it had very high TPSA (186.37 Å²) and low drug-likeness scores (Table 4), indicating poor membrane permeability and limited pharmacokinetic potential. M02, M03, and M04 showed similar physicochemical features, including moderate TPSA (97.99-110.38 Å²), low rotatable bond counts, and balanced hydrogen-bonding capacity, indicating acceptable flexibility and membrane transport ability. Compound M03, having a slightly higher molecular weight (488.7 Da), exhibited a more hydrophobic physicochemical profile (LogP=4.34) and moderate TPSA (97.99 Å²), which signifies adequate lipophilicity and favourable diffusion potential through lipid membranes (Wang et al., 2021).

Zenarestat indicated a well-balanced profile consistent with drug-like standards, including moderate lipophilicity (LogP=3.35). Notably, M01's compound has a notably negative LogP (-0.32), underscoring its hydrophilic nature, which, together with its high TPSA, explains its reduced permeability. Therefore, M02, M03, and M04 displayed the most promising physicochemical behaviour, whereas M01 likely requires structural optimisation to improve permeability and drug likeness. It also contains a glucose moiety, which may enhance solubility.

Table 4: Pharmacokinetic properties and drug-likeness of the top selected compounds and the reference ligand Zenarestat

	Parameters	Eriodictyol-7-O-Glucoside (M01)	(-)-Epicatechin (M02)	Euscaphic Acid (M03)	Catechin (M04)	Native Ligand (Zenarestat)
Pharmacokinetics	GI absorption	Low	High	High	High	High
	BBB permeability	No	No	No	No	No
	P-gp substrate	Yes	Yes	Yes	Yes	No
	CYP1A2 inhibitor	No	No	No	No	Yes
	CYP2C19 inhibitor	No	No	No	No	Yes
	CYP2C9 inhibitor	No	No	No	No	Yes
	CYP2D6 inhibitor	No	No	No	No	No
	CYP3A4 inhibitor	No	No	No	No	No

Drug-likeness	Lipinski Rule	No	Yes	Yes	Yes	Yes
	Bioavailability Score	0.17	0.55	0.56	0.55	0.56
Medicinal Chemistry	PAINS	1	1	0	1	0
	Brenk	1	1	1	1	0
	Synthetic accessibility	5.05	3.5	6.59	3.5	2.61

Together, these pharmacokinetic predictions refined the suitability of the hit candidate for further validation. M02, M03, and M04 displayed high gastrointestinal (GI) absorption, consistent with optimal oral bioavailability, whereas M01 showed low GI absorption, consistent with its high polarity and poor permeability observed in Table 4. Blood-brain barrier (BBB) permeability was not displayed by the hit compounds nor by the native ligand. This can be considered a positive feature for potential drug development (Dong et al., 2022). All four hit compounds were recognised as P-glycoprotein (P-gp) substrates, which may limit intracellular accumulation due to efflux activity and thereby reduce their effective concentration at the active site.

In contrast, Zenarestat was not identified as a P-gp substrate, possibly contributing to its improved bioavailability. So, all top molecules (M01-M04) could significantly impact their gastrointestinal absorption and distribution. Although M02 and M04 showed high GI absorption, their classification as P-gp substrates suggests they may be subject to efflux, thereby reducing their bioavailability (Miyake et al., 2021). The phytochemicals demonstrated a favourable metabolic safety profile, with no inhibition of major cytochrome P450 isoforms, resulting in a low likelihood of drug interactions. In contrast, the reference ligand Zenarestat inhibited CYP1A2, CYP2C19, and CYP2C9, indicating a higher risk of metabolic interference compared with the natural molecules.

Drug-likeness analysis further reinforced the suitability of M02, M03, and M04, all of which met Lipinski's Rule of Five criteria, whereas M01 violated the criteria, again reflecting its high polar surface area and hydrogen-bonding burden. Bioavailability scores showed a similar trend, with M01 having the lowest value (0.17), compared to ~0.55-0.56 for the other phytocompounds and Zenarestat.

Medicinal chemistry screened PAINS and Brenk alerts in most of the selected phytochemicals, consistent with their plant-derived structural complexity, while Zenarestat displayed no alerts, supporting its optimised synthetic design. Synthetic accessibility scores highlighted M03 as the most complex to synthesise (6.59), whereas Zenarestat was found to be the most synthetically tractable (2.61), showing typical differences between natural scaffolds and established pharmaceuticals.

Table 5: Toxicity profile of the four top and native ligands

Toxicity Parameters	**Eriodictyol-7-O-Glucoside (M01)**	**(-)-Epicatechin (M02)**	**Euscaphic Acid (M03)**	**Catechin (M04)**	**Native Ligand (Zenarestat)**
Predicted LD_{50} (mg/mL)	12000	10000	2000	10000	4250
Toxicity class	6	6	4	6	5
Hepatotoxicity	Inactive	Inactive	Inactive	Inactive	Inactive
Neurotoxicity	Inactive	Inactive	Inactive	Inactive	Active
Nephrotoxicity	Active	Active	Inactive	Active	Active
Cardiotoxicity	Inactive	Inactive	Active	Inactive	Inactive
Immunotoxicity	Active	Inactive	Active	Inactive	Active
Mutagenicity	Inactive	Inactive	Inactive	Inactive	Inactive
Cytotoxicity	Inactive	Active	Inactive	Inactive	Inactive

The ProTox-III toxicity assessment tool predicted thatD_{50} indicated that M01 (12,000 mg/kg), M02 (10,000 mg/kg), and M04

(10,000 mg/kg) belong to toxicity class 6, representing the least toxic compounds (Banerjee et al., 2024). Notably, M03 exhibited a lower LD_{50} of 2,000 mg/kg (class 4), indicating moderate toxicity, while the native ligand Zenarestat showed mild toxicity (LD_{50}=4,250 mg/kg; class 5). The comparatively high LD50s of M01, M02, and M04 thus suggest higher safety profiles than those of both M03 and Zenarestat, underscoring their potential for safer pharmacological development.

All hit molecules were indicated as non-hepatotoxic and non-mutagenic in organ-specific predictions, with negligible risks of hepatic injury and genotoxicity, which is favourable for long-term therapeutic application (Kozlov et al., 2025). Neurotoxicity was detected only with Zenarestat, while all four hit molecules were neuro-inactive, emphasising their potential to avoid central nervous system side effects. M01, M02, M04, and Zenarestat displayed nephrotoxicity, whereas M03 was anticipated to be renal inactive. It was observed that compounds with polyphenolic scaffolds exhibit mild renal toxicity, warranting further investigation using renal biomarker assays. Immunotoxicity was observed in M01, M03, and Zenerastat, whereas M02 and M04 were predicted to be immune-inactive, signifying possible structural differences influencing immune modulation (Barratt, 2000). In contrast, cardiotoxicity was only displayed in M03, correlating with its moderate toxicity class and emphasising potential cardiac safety concerns. Cytotoxicity was detected only with the M04 molecule.

In comparison, M01, M02, and M04 reflected the most favourable toxicity profiles, characterised by high LD_{50} values, less organ toxicity, and acceptable ADME properties. However, M03, with strong docking affinity, reflected relatively higher toxicity risks. Compared with Zenarestat, three of the four phytocompounds showed lower acute and organ-specific toxicities, supporting their potential as safer natural AR inhibitors.

In general, molecules M02 and M04 presented favourable pharmacokinetics, drug-likeness, and pharmacodynamics profiles comparable to those of the reference scaffolds, while M01 showed limited oral drug potential due to poor permeability and rule-based violations, despite falling within the minimal toxicity class. M03 was identified as the most toxic among the top four compounds, along with Zenarestat. It served as a reference model with optimised medicinal chemistry characteristics but remarkable CYP inhibition liability. All these results indicate M02 and M04 as potential hit candidates for further development, whereas M01 and M03 may require rational structural refinement to improve their pharmacokinetic suitability and reduce toxicity.

The ADME and toxicity predictions indicated that the phytocompounds derived from *Z. budhensis* exhibit encouraging drug-likeness and safety characteristics, particularly compared with Zenarestat. Overall, this study highlighted the need for further stability assessment of the complexes using advanced computational tools, along with the predicted nephrotoxicity and immunotoxicity of the compounds, and called for experimental validation, including an *in vitro* cytotoxicity assay.

Conclusions

The above study examined the binding potential of phytocompounds from *Z. budhensis* leaves to the aldose reductase enzyme (AR) (PDB ID: 1IEI) using molecular docking, drug-likeness assessment, and ADMET predictions. The study revealed that four compounds Eriodictyol-7-O-glucoside (M01), Epicatechin (M02), Euscaphic acid (M03), and Catechin (M04) interacted strongly within the active site of the AR with docking scores of -11.3, -10.3, -10.1, and -9.9 kcal/mol, respectively, which also advise their possible role in regulating glucose utilisation than that of the native ligand Zenarestat (-9.7 kcal/mol). They were identified as potential candidates based on their binding affinities, numerous hydrogen-bonding interactions, and favourable pharmacokinetic properties. ADMET predictions confirmed that two molecules (M02 and M04) demonstrate the best characteristics of drug-likeness, oral bioavailability, and physicochemical balance, supporting their potential as safe (least toxic) and possible natural modulators of AR compared to Zenarestat. To confirm the identified hit compounds' biological efficacy and safety, molecular dynamics simulations, *in vitro* enzymatic inhibition tests, and *in vivo* bio-investigations are recommended in the future. Overall, this study provides a computational foundation for developing plant-based therapeutic agents to address metabolic complications of diabetes associated with AR dysfunction.

Acknowledgements

The author would like to express gratitude to the Research Directorate, Office of the Rector, Tribhuvan University, Kirtipur, Kathmandu, for providing a PhD Thesis Grant through the Research Endowment Fund (REF).

References

Agu, P. C., Afiukwa, C. A., Orji, O. U., Ezeh, E. M., Ofoke, I. H., Ogbu, C. O., Ugwuja, E. I., & Aja, P. M. (2023). Molecular docking as a tool for the discovery of molecular targets of nutraceuticals in diseases management. *Scientific Report*, *13*(1), 1–18. https://doi.org/10.1038/s41598-023-40160-2

Alam, F., Shafique, Z., Amjad, S. T., & Bin Asad, M. H. H. (2019). Enzymes inhibitors from natural sources with antidiabetic activity: A review. *Phytotherapy Research*, *33*(1), 41–54. https://doi.org/10.1002/PTR.6211

Alam, S., Sarker, M. M. R., Sultana, T. N., Chowdhury, M. N. R., Rashid, M. A., Chaity, N. I., Zhao, C., Xiao, J., Hafez, E. E., Khan, S. A., & Mohamed, I. N. (2022). Antidiabetic Phytochemicals From Medicinal Plants: Prospective Candidates for New Drug Discovery and Development. *Frontiers in Endocrinology*, *13*, 800714. https://doi.org/10.3389/FENDO.2022.800714/FULL

Ashik, M. A., Islam, T., Fujii, M., Alam, M. M., & Hossain, M. N. (2022). Interaction pattern of aldose reductase with β-glucogallin: Active site exploration and multiple docking analyses. *Informatics in Medicine Unlocked*, *30*, 100938. https://doi.org/10.1016/J.IMU.2022.100938

Banerjee, P., Kemmler, E., Dunkel, M., & Preissner, R. (2024). ProTox 3.0: a webserver for the prediction of toxicity of chemicals. *Nucleic Acids Research*, *52*(W1), W513–W520. https://doi.org/10.1093/NAR/GKAE303

Barratt, M. D. (2000). prediction of toxicity from chemical structure. *Cell Biology and Toxicology*, *16*(1), 1–13. https://doi.org/10.1023/A:1007676602908

Berman, H. M., Westbrook, J., Feng, Z., Gilliland, G., Bhat, T. N., Weissig, H., Shindyalov, I. N., & Bourne, P. E. (2000). The Protein Data Bank. *Nucleic Acids Research*, *28*(1). https://doi.org/10.1093/nar/28.1.235

Bharati, S., Maharjan, B., Shrestha, T., Shrestha, S. S., Sut, S., Devkota, H. P., Shrestha, R. L. S., & Dall'Acqua, S. (2025). LC-DAD-MS^n and HR-LC-QTOF Analysis of *Ziziphus budhensis* Leaves and Evaluation of Their *In Vitro* and *In Vivo* Biological Activities. *Chemistry and Biodiversity*, *22*(8), e202402835. https://doi.org/10.1002/CBDV.202402835

Biovia DS (2021) Discovery studio visualiser v21. 1.0. 20298. *San Deigo Dassualt Systemes., 2021*.

Butler, M. S. (2004). The role of natural product chemistry in drug discovery. *Journal of Natural Products*, *67*(12), 2141–2153. https://doi.org/10.1021/np040106y

Cao, D., Wang, J., Zhou, R., Li, Y., Yu, H., & Hou, T. (2012). ADMET evaluation in drug discovery. 11. PharmacoKinetics Knowledge Base (PKKB): A comprehensive database of pharmacokinetic and toxic properties for drugs. *Journal of Chemical Information and Modeling*, *52*(5), 1132–1137. https://doi.org/10.1021/ci300112j

Chandrasekhar, V., Rajan, K., Kanakam, S. R. S., Sharma, N., Weiβenborn, V., Schaub, J., & Steinbeck, C. (2025). COCONUT 2.0: a comprehensive overhaul and curation of the collection of open natural products database. *Nucleic Acids Research*, *53*(D1), D634–D643. https://doi.org/10.1093/NAR/GKAE1063

Daina, A., Michielin, O., & Zoete, V. (2017). SwissADME: A free web tool to evaluate pharmacokinetics, drug-likeness and medicinal chemistry friendliness of small molecules. *Scientific Reports*, *7*. https://doi.org/10.1038/srep42717

Del-Corso, A., Balestri, F., Di Bugno, E., Moschini, R., Cappiello, M., Sartini, S., La-Motta, C., Da-Settimo, F., & Mura, U. (2013). A New Approach to Control the Enigmatic Activity of Aldose Reductase. *PLOS ONE*, *8*(9), e74076. https://doi.org/10.1371/JOURNAL.PONE.0074076

Demain Arnold L., & Zhang Lixin. (2019). *Natural Products: Drug Discovery and Therapeutic Medicine*. Humana Press, Totowa, New Jersey.

Dong, M., Wen, S., & Zhou, L. (2022). The Relationship Between the Blood-Brain-Barrier and the Central Effects of Glucagon-Like Peptide-1 Receptor Agonists and Sodium-Glucose Cotransporter-2 Inhibitors. *Diabetes, Metabolic Syndrome and Obesity*, *15*, 2583-2597. https://doi.org/10.2147/DMSO.S375559

Greene, D. A., Arezzo, J. C., & Brown, M. B. (1999). Effect of aldose reductase inhibition on nerve conduction and morphometry in diabetic neuropathy. *Neurology*, *53*(3), 580–591. https://doi.org/10.1212/WNL.53.3.580

Guedes, I. A., Barreto, A. M. S., Marinho, D., Krempser, E., Kuenemann, M. A., Sperandio, O., Dardenne, L. E., & Miteva, M. A. (2021). New machine learning and physics-based scoring functions for drug discovery. *Scientific Report*, *11*(1), 1–19. https://doi.org/10.1038/s41598-021-82410-1

Guedes, I. A., de Magalhães, C. S., & Dardenne, L. E. (2014). Receptor-ligand molecular docking. *Biophysical Reviews*, *6*(1), 75–87. https://doi.org/10.1007/s12551-013-0130-2

Gupta, J. K. (2024). The Role of Aldose Reductase in Polyol Pathway: An Emerging Pharmacological Target in Diabetic Complications and Associated Morbidities. *Current Pharmaceutical Biotechnology*, *25*(9), 1073–1081. https://doi.org/10.2174/1389201025666230830125147

Hanwell, M. D., Curtis, D. E., Lonie, D. C., Vandermeerschd, T., Zurek, E., & Hutchison, G. R. (2012). Avogadro: An advanced semantic chemical editor, visualisation, and analysis platform. *Journal of Cheminformatics*, *4*(8). https://doi.org/10.1186/1758-2946-4-17

Hefti, F. F. (2008). Requirements for a lead compound to become a clinical candidate. *BMC Neuroscience*, *9*(3), 1–7. https://doi.org/10.1186/1471-2202-9-S3-S7

Kim, S., Chen, J., Cheng, T., Gindulyte, A., He, J., He, S., Li, Q., Shoemaker, B. A., Thiessen, P. A., Yu, B., Zaslavsky, L., Zhang, J., & Bolton, E. E. (2023). PubChem 2023 update. *Nucleic acid research, 51*(2022), 1373–1380.

Kitchen, D. B., Decornez, H., Furr, J. R., & Bajorath, J. (2004). Docking and scoring in virtual screening for drug discovery: Methods and applications. *Nature Reviews Drug Discovery, 3*(11). https://doi.org/10.1038/nrd1549

Kozlov, D. S., Rodimova, S., Filatov, P., Mozherov, A., Timashev, P. S., Zyuzin, M. V., & Kuznetsova, D. S. (2025). Genomic medicine in hepatology: mechanisms and liver treatment strategies. *Molecular Medicine*, *31*(1), 302. https://doi.org/10.1186/S10020-025-01358-4

Miyake, T., Tsutsui, H., Haraya, K., Tachibana, T., Morimoto, K., Takehara, S., Ayabe, M., Kobayashi, K., & Kazuki, Y. (2021). Quantitative prediction of P-glycoprotein-mediated drug–drug interactions and intestinal absorption using humanized mice. *British Journal of Pharmacology*, *178*(21), 4335-4351. https://doi.org/10.1111/bph.15612

Nauck, M. A., Wefers, J., & Meier, J. J. (2021). Treatment of type 2 diabetes: challenges, hopes, and anticipated successes. *The Lancet Diabetes and Endocrinology 9*(8). https://doi.org/10.1016/S2213-8587(21)00113-3

Osbourn, A. E., & Lanzotti, V. (2009). Plant-derived natural products: Synthesis, function, and application. *Plant-derived Natural Products: Synthesis, Function, and Application, 6*. https://doi.org/10.1007/978-0-387-85498-4

Pasquel, F. J., Lansang, M. C., Dhatariya, K., & Umpierrez, G. E. (2021). Management of diabetes and hyperglycaemia in the hospital. *The Lancet Diabetes and Endocrinology*, *9*(3), 174–188. https://doi.org/10.1016/S2213-8587(20)30381-8

Ramasamy, R., & Goldberg, I. J. (2010). Aldose Reductase and Cardiovascular Diseases, Creating Human-Like Diabetic Complications in an Experimental Model. *Circulation Research*, *106*(9), 1449–1458. https://doi.org/10.1161/CIRCRESAHA.109.213447

Shrestha, R. L. S., Parajuli, N., Neupane, P., Dhital, S., Maharjan, B., Shrestha, T., Bharati, S., Marasini, B. P., & Adhikari Subin, J. (2024). A Computational Approach of Antidiabetic Potential Evaluation of Flower and Seed of Nyctanthes arbor tristis Linn. *Turkish Computational and Theoretical Chemistry*, *9*(1), 1–18. https://doi.org/10.33435/tcandtc.1487560

Shrestha, R. L. S., Tamang, A., Poudel, M., Shiva, M. C., Parajuli, N., Shrestha, A., Shrestha, T., Bharati, S., Maharjan, B., Marasini, B. P., & Subin, J. A. (2025a). Unveiling the therapeutic potential of artopetelin flavonoids through computational approaches as peroxisome proliferator-activated receptor-delta (PPARδ) agonists. *Journal of Molecular Graphics and Modelling*, *140*. https://doi.org/10.1016/j.jmgm.2025.109105

Shrestha, R. L. S., Poudel, M., Tamang, A., M.C., S., Parajuli, N., Shrestha, A., Shrestha, T., Bharati, S., Maharjan, B., Marasini, B. P., Subin, J. A (2025b). Exploring *Artocarpus heterophyllus* phytochemicals as novel mineralocorticoid receptor inhibitors: A computational approach to hypertension therapy. *Journal of King Saud University – Science*, *37*, 1–7. https://doi.org/10.25259/JKSUS_370_2025

Shrestha, R. L.S., Tamang, A., Chhetri, S. P., Parajuli, N., Poudel, M., Shiva, M. C., Shrestha, A., Shrestha, T., Bharati, S., Maharjan, B., Marasini, B. P., & Subin, J. A. (2025c). AI-assisted discovery of potent FGFR1 inhibitors *via* virtual screening and in silico analysis. *PLOS ONE*, *20*(9), e0331837. https://doi.org/10.1371/JOURNAL.PONE.0331837

Subin, J. A., & Shrestha, R. L. S. (2024). Computational Assessment of the Phytochemicals of Panax ginseng C.A. Meyer Against Dopamine Receptor D1 for Early Huntington's Disease Prophylactics. *Cell Biochemistry and Biophysics*, *82*, 3413–3423. https://doi.org/10.1007/s12013-024-01426-2

Trott, O., & Olson, A. J. (2010). AutoDock Vina: Improving the speed and accuracy of docking with a new scoring function, efficient optimisation, and multithreading. *Journal of Computational Chemistry*, *31*(2). https://doi.org/10.1002/jcc.21334

Wang, S., König, G., Roth, H. J., Fouché, M., Rodde, S., & Riniker, S. (2021). Effect of Flexibility, Lipophilicity, and the Location of Polar Residues on the Passive Membrane Permeability of a Series of Cyclic Decapeptides. *Journal of Medicinal Chemistry*, *64*(17), 12761–12773. https://doi.org/10.1021/ACS.JMEDCHEM.1C00775

Xie, Z. R., & Hwang, M. J. (2010). An interaction-motif-based scoring function for protein-ligand docking. *BMC Bioinformatics*, *11*(1), 1–16. https://doi.org/10.1186/1471-2105-11-298

Xue, M., Liu, B., Cao, S., & Huang, X. (2025). FeatureDock for protein-ligand docking guided by physicochemical feature-based local environment learning using transformer. *Npj Drug Discovery*, *2*(1), 1–12. https://doi.org/10.1038/s44386-025-00005-6

Yuan, S., Chan, H. C. S., & Hu, Z. (2017). Using PyMOL as a platform for computational drug design. In *Wiley Interdisciplinary Reviews: Computational Molecular Science*, 7(2). https://doi.org/10.1002/wcms.1298